

Using on-nadir spectral reflectance to detect soil surface changes induced by simulated rainfall and wind tunnel abrasion

Adrian Chappell,^{1*} Ted M. Zobeck² and Gillian Brunner¹

¹ School of Environment & Life Sciences, University of Salford, Manchester, M5 4WT, UK

² USDA, Agricultural Research Service, Cropping Systems Research Laboratory, Lubbock, Texas 79415, USA

*Corresponding to: A. Chappell,
School of Environment and Life
Sciences, University of Salford,
Manchester, M5 4WT, UK.
E-mail: a.chappell@salford.ac.uk

Abstract

The surface susceptibility to erosion (erodibility) is an important component of soil erosion models. Many studies of wind erosion have shown that even relatively small changes in surface conditions can have a considerable effect on the temporal and spatial variability of dust emissions. One of the main difficulties in measuring erodibility is that it is controlled by a number of highly variable soil factors. Collection of these data is often limited in scale because *in situ* measurements are labour-intensive and very time-consuming. To improve wind erosion model predictions over several spatial and temporal scales simultaneously, there is a requirement for a non-invasive approach that can be used to rapidly assess changes in the compositional and structural nature of a soil surface in time and space. Spectral reflectance of the soil surface appears to meet these desirable requirements and it is controlled by properties that affect the soil erodibility.

Three soil surfaces were modified using rainfall simulation and wind tunnel abrasion experiments. Observations of those changes were made and recorded using digital images and on-nadir spectral reflectance. The results showed clear evidence of the information content in the spectral domain that was otherwise difficult to interpret given the complicated interrelationships between soil composition and structure. Changes detected at the soil surface included the presence of a crust produced by rainsplash, the production of loose erodible material covering a rain crust and the selective erosion of the soil surface. The effect of rainsplash and aeolian abrasion was different for each soil tested and crust abrasion was shown to decrease as rainfall intensity increased. The relative contributions of the eroded material from each soil surface to trapped mixtures of material assisted the erodibility assessment. Ordination analyses within each of two important soil types explained significant amounts of the variation in the reflectance of all wavebands by treatments of the soil and hence changes in the soil surface. The results show that soil surface conditions within a soil type are an underestimated source of variation in the characterization of soil surface erodibility and in the remote sensing of soil. Copyright © 2005 John Wiley & Sons, Ltd.

Keywords: wind erosion; soil erodibility; wind tunnel; rainfall simulator; on-nadir spectral reflectance; canonical ordination; redundancy analysis; linear mixture modelling

Received 4 March 2004;
Revised 6 August 2004;
Accepted 3 September 2004

Introduction

Soil erosion by wind and water involves the interaction of a complex set of physical and chemical processes governed by many factors. These factors are commonly divided between *erosivity*, the potential of the fluid to erode the surface, and *erodibility*, the degree to which the surface is susceptible to this erosivity. Many studies have focused on erosivity to model simply soil erosion over large areas. For example, wind erosion indices have been used to model the wind erosion potential in Australia (Kalma *et al.*, 1988; Burgess *et al.*, 1989; McTainsh *et al.*, 1990, 1998). These studies assume that variation in surface erodibility is static in time and/or in space. One of the first attempts to account for variation in erosivity and erodibility was the wind erosion equation (Woodruff and Siddoway, 1965) that used empirical relationships derived from experimental studies. Similar experimental approaches continue to be used for wind

erosion assessment (Gillette and Hanson, 1989; Nickling and Gillies, 1993) because they elucidate the processes controlling wind erosion. Increased understanding of erosivity from these experiments led to the development of wind erosion models which use physically based explanations of aeolian processes that are more generally applicable (e.g. Marticorena and Bergametti, 1995; Shao *et al.*, 1996; Fryrear *et al.*, 1998; Böhner *et al.*, 2003).

Erodibility has received somewhat less attention when compared to erosivity, perhaps due to problems concerning its accurate measurement. Geeves *et al.* (2000) contend that in many cases this has led to a misunderstanding of the concept and that erodibility should be viewed as a dynamic continuum rather than a stable property of the soil surface. One of the main difficulties in measuring erodibility is that this property is controlled by a number of soil factors that may vary considerably in space and time. Field studies of erodibility are typically conducted on tilled agricultural soils (e.g. Zobeck, 1991b). However, Chappell *et al.* (2003) have shown that, typically, spatial and temporal samples of saltation flux do not have the same spatial scale as those of several properties known to control soil surface erodibility by wind. Detailed studies of soil surface erodibility have been conducted using portable field wind tunnels (e.g. Nickling and Gillies, 1993). Nickling *et al.* (1999) reviewed studies of dust emissions from agricultural and natural surfaces and showed that dust flux in natural field conditions was not a simple function of shear velocity and saltation flux which was thought to be the case in idealized wind tunnel experiments. Data from these studies represented a wide range of soil types and surface conditions and showed considerable scatter in dust fluxes for similar wind speeds, even at the same site. The authors suggested that their results indicated that even relatively small changes in surface conditions can have an effect on the temporal and spatial variability of dust emissions at a given site.

Textural, mineralogical and chemical characteristics of the surface are critical to the understanding of aeolian processes. Quantitative measures of the effects of these soil surface characteristics on dust emissions are essential for wind erosion model development. Recent developments in models of the dust cycle (e.g. Sokolik and Toon, 1996) and wind erosion (Shao and Leslie, 1997) have also highlighted the need for information on the spatial and temporal variation of soil surface conditions because soil surface conditions such as composition, aggregation and roughness control the surface susceptibility to wind erosion and hence the emission of dust (Zobeck, 1991b). Shao *et al.* (1996) suggested that the main limitation of wind erosion models is their inability to incorporate the evolution of surface soil conditions. The soil sub-model in the USDA-Agricultural Research Service, Wind Erosion Prediction System (WEPS) model was developed in recognition that the soil's aggregation and surface state can dramatically affect erodibility (Hagen *et al.*, 1995). Collection of these data, even in the USA, is often limited to the field/regional scale because *in situ* measurements are labour-intensive and very time-consuming and experiments to understand the spatial and temporal variation of erodibility over several scales are prohibitively expensive. Arguably, these field-based approaches are even inadequate at the field scale where soil surface conditions vary considerably and evolve simultaneously in space and time. The scale of measurement may be second to the difficulty of making a measurement of the soil surface. Soil samples bulked over depth provide a very crude estimate of the soil surface susceptibility to wind erosion (erodibility). Unfortunately, the relationship between a bulked soil sample and the soil surface may be at worst flawed by interference with the surface during the measurement process, at best strongly dependent on the inferences made about how representative the sample is of the soil surface, and further complicated by the implicit assumption that the relationship remains constant over time.

Shao *et al.* (1996) provided one of the first physically based wind erosion models to operate over scales from the field to the continent (Australia). One of the main reasons for its success over several scales was the inclusion of remote sensing data. Shao and Leslie (1997) suggested that the Shao *et al.* (1996) model required more detailed estimation of erodibility, in particular the estimation of surface roughness elements, soil moisture content and surface crusting. They suggested that the dynamic effect of surface roughness elements is difficult to describe because surfaces are often composed of standing roughness elements, flat surface covers, tillage ridges and various levels of random roughness elements (Potter *et al.*, 1990). An accurate assessment of land surface parameters is essential for global dust cycle models and its linkage to climate change (Sokolik and Toon, 1996).

To improve wind erosion model predictions over several spatial and temporal scales simultaneously, there is a requirement for a non-invasive approach that can be used to rapidly assess changes in the compositional and structural nature of a soil surface in time and space. This requirement is consistent with recent work on soil crusts and infiltration and its attendant implications for soil erosion (Goldshleger *et al.*, 2001; Ben-Dor *et al.*, 2003). Furthermore, the required approach for erosion should provide a holistic framework so that the factors controlling the processes of erodibility may be considered on the same continuum (Geeves, *et al.*, 2000). The key to providing this information is that light (in the visible and infrared region) reflected from a soil surface is directly related to its biophysical and geometric characteristics (Irons *et al.*, 1989). The characteristics of electromagnetic radiation are altered when radiation interacts with matter. These alterations are a function of the composition and structure of the matter and hence observations of soil reflectance can provide essential information on the condition of the soil surface (Ben-Dor *et al.*, 1999).

Measurements of the intrinsic optical properties of the soil surface produce wavelength-specific absorption of electromagnetic radiation, yielding diagnostic reflectance spectra for the properties under investigation. The main controls on its variation – organic matter, soil moisture, mineralogy, particle size and surface roughness (Price, 1990; Heute and Escadafel, 1991) – are also those that affect (either directly or indirectly) the surface soil erodibility by wind. Thus, there is a strong potential for developing a physical relationship between spectral reflectance and erodibility (e.g. Latz *et al.*, 1984; Baumgardner *et al.*, 1985). Non-wavelength-specific or structural soil factors such as roughness can be deduced from spectral data by examining the reflectance at all possible illumination and sensor view angles of a particular target as represented by the bi-directional reflectance distribution function (BRDF) (Jacquemoud *et al.*, 1992). Analysis of the structural components of the experiments is beyond the scope of this paper.

There has been a considerable amount of work published on soil reflectance that remains unfamiliar to workers in geomorphology, partly because of the time-consuming nature of operating across disciplines and because of the difficulty in overcoming technological jargon found in most specialist research areas. The aim here is to compare judiciously the main findings of that literature with the results of process-based laboratory experiments performed to (1) examine the composition of three soils using soil reflectance data and (2) characterize soil surface change in composition under controlled rainfall, drying and wind tunnel experiments.

Methods

Spectral reflectance measurement

A comprehensive discussion of reflectance and a detailed review of the micro- and macro-scopic interactions of solar energy and soil can be found elsewhere (Nicodemus *et al.*, 1977; Irons *et al.*, 1989; Ben-Dor *et al.*, 1999). Perhaps as a consequence of such a well established background to spectral reflectance, many studies have included empirical laboratory and simulation experiments to predetermined physical and chemical conditions (composition) of soil surfaces. There are far fewer studies that have applied this approach to the relationship between surfaces degraded by water erosion and changes in surface spectral reflectance (e.g. Latz *et al.*, 1984; Baumgardner *et al.*, 1985). Most laboratory and field experiments on soil spectral reflectance have naturally focused on bare soil because of the ease with which change at the soil surface may be detected. As a consequence, many investigations have taken place in arid and semi-arid regions where vegetation is sparse. However, in recent years there has been an increasing awareness of the importance of reflectance for biophysical and chemical interactions of microphytic (cyanobacterial) crusts (e.g. Karnieli *et al.*, 1999) that render the surface no longer 'bare'. This last development illustrates the complexity of establishing simple relationships between the composition of the soil surface and the soil spectral reflectance.

Spectrometers offer increased precision and have been used successfully for soil studies (Milton *et al.*, 1995). The Analytical Spectral Devices (ASD) spectroradiometer used here had a spectral range of 350–2500 nm and spectral sampling of 1.4 nm between 350 and 1050 nm and 2 nm between 1000 and 2500 nm. An 8° field of view was used and illumination was provided by a 1000 W halogen lamp which was held constant at 53° above the horizontal soil plane. As part of a larger project on erodibility, a goniometer was used to allow repeatable and consistent measurements of multi-angular reflectance (including on-nadir) of the soil surface from a constant height (35 cm) and provided view zenith angles. Several illumination azimuth angles were considered as part of the larger project and consequently multiple on-nadir reflectance measurements were made. The average of those on-nadir measurements was used here. The radiometer had a video camera strapped to it so that images of the soil surface were also captured at the same time as on-nadir reflectance to provide a visual record of changes to the soil surface composition and structure during the experiments. The soil surfaces were placed under the sensors at exactly the same location so that reflectance from the soil surface was the same during each on-nadir measurement. A calibrated spectralon panel provided total irradiance information. A spectralon reflectance reference measurement was made immediately before the target measurement under the same conditions as the measurement. Finally, conversion to spectral reflectance was conducted by dividing the radiance spectra of the soil samples by the radiance spectrum of the white spectralon reference panel. Some small hiatuses occurred in the reflectance spectra at the interface between the fibre-optics of the sensor (around 1000 nm and 1800 nm) and these were not smoothed or manipulated for presentation.

Soil types and property measurements

Three soil types were used in the experiments and Table I provides some of their characteristics and their sample locations. The soil types chosen were susceptible to wind erosion on agricultural land that was close to where the

Table I. Some characteristics of the soils used in the experiments (see text for soil type and measurement details)

Soil type (label) and location	Soil Munsell Dry Colour	Fe (III) (%)	pH	Organic carbon content (%)	Median particle size (μm)	Sand content (%)	Silt content (%)	Clay content (%)
Amarillo fine sand (FS) (N 33° 33·82' W 101° 35·37')	7·5YR 5/6	0·26	7·53 \pm 0·034	0·34 \pm 0·008	176·2	89·1	4·0	6·9
Amarillo fine sandy loam (FSL) (N 33° 35·67' W 101° 54·07')	7·5YR 4/4	0·53	7·99 \pm 0·005	0·83 \pm 0·091	88·3	63·4	18·2	18·4
Randall clay loam (CL) (N 33° 38·07' W 101° 3·67')	7·5YR 5/2	0·55	7·07 \pm 0·005	1·09 \pm 0·010	43·4	44·9	22·7	32·4
Abrader sand (ABS)	10YR 7/2	—	—	—	728·9	100	0	0

—, No data

experiments were conducted in the vicinity of the United States Department of Agriculture (USDA) Agricultural Research Service (ARS) in Lubbock, Texas. The soil types were also used to represent the variation in texture, an important factor controlling the wind erosion. The first type (FS) was an Amarillo fine sand, that was a fine, mixed, superactive, thermic Aridic Paleustalf. The second (FSL) was an Amarillo fine sandy loam. The third soil type (CL) was a Randall clay loam which was a fine, smectitic, thermic Ustic Epiaquert. All of the soils were from the Ap horizon. An abrader was used in the wind tunnel experiments and the characteristics of this material are also shown in Table I.

The total organic carbon was measured by dry combustion of air-dried (ground to $<180\ \mu\text{m}$) soil in a Vario Max-ELEMENTAR CN-analyser (D-63452 Hanau, Germany). The pH of the soils was measured in a 1:1 soil:water mixture. The dispersed particle size distribution of each soil (Table I) was measured using a Coulter LS230 laser particle sizer. The LS230 was calibrated to similar soils that had been analysed using the pipette method (Zobeck, 2003). To disperse the soils, approximately 300 mg of each soil were placed in a 20 ml plastic bottle filled with 10 ml of hexametaphosphate (Calgon) solution ($50\ \text{g l}^{-1}$) and shaken overnight using a reciprocating shaker. The Fe(III) measured was the stable form measured using dithionite-citrate.

Soil treatment experiments

Straightforward experiments involving a rainfall simulator, drying ovens and a wind tunnel were used to illustrate differences in soil material and soil surfaces during a process. The experiments were designed so that the effect on the soil was predictable but the spectral reflectance of the soil was not well understood. The approach was developed to include simulations of natural environmental processes that were known to alter the soil surface (erodibility) condition. This provided an alternative to the traditional development of a relationship between soil properties and spectral wavebands.

In preparation for the process-based experiment, all soils (FS, FSL and CL) were passed through a 2 mm mesh and loaded into 2507 cm² sample trays (54·5 cm \times 46 cm). The tray bases comprised wire mesh and muslin material to allow water drainage whilst minimizing soil loss. The tray sides were adjustable and were standardized at a thickness of 6·5 cm during the loading process. The sides were lowered during the experiments to account for surface lowering during wind erosion. A straight-edge was used to smooth the surface and remove initial inconsistencies between soils and individual trays. Three replicate trays for each of the three soils were prepared for each of the two experiments (total of 18 trays). The intention was to expose each soil type to simulations of short and long duration of abrasion for high and low intensity rainfall (Table II). Unfortunately, operational constraints reduced the experiments that were performed on the CL soil to only high rainfall intensity (Table II).

Following on-nadir reflectance measurements (as described above) all trays were subjected to the rainfall simulator (Norton and Brown, 1992), using a Veejet 80 100 nozzle, which produced rainfall energy of approximately $20\ \text{J m}^{-2}\ \text{mm}^{-1}$ (Baumhardt *et al.*, 1990). This rainfall energy was similar to that applied in experiments by Ben-Dor *et al.* (2003). Soil trays were exposed to either a high rainfall intensity simulation at $94\ \text{mm h}^{-1}$ with a cumulative rainfall amounting to 19 mm or low rainfall intensity at $31\ \text{mm h}^{-1}$ with the same total amount of rainfall. During the rainfall simulations all trays were placed on a level metal frame approximately 30 cm above the ground to allow soil water drainage and uniform percolation of the soil water through the soils. The trays were allowed to drain for 30 minutes to reduce liquefaction processes during transportation to the ovens for drying. The ovens were set at $40\ ^\circ\text{C}$

Table II. Intensity and duration of rainfall and wind abrasion treatments applied to each of the soil types (see text for details)

Soil type	Treatment					
	None ^a	Low ^b rain and dry	1 min abrasion	8 min abrasion	High ^c rain and dry	1 min abrasion 8 min abrasion
FS	X	X	X	X	X	X X
FSL	X	X	X	X	X	X X
CL	X				X	X X

^a Both low rainfall and high rainfall intensity experiments included trays with no rainfall

^b High intensity rainfall was simulated at 94 mm h⁻¹ with a cumulative rainfall of 19 mm

^c High intensity rainfall was simulated at 31 mm h⁻¹ with a cumulative rainfall of 19 mm

and the trays remained in the ovens for 45 hours to ensure surface layers were dry. After they were removed from the ovens, the trays were allowed to cool overnight. On-nadir reflectance was measured once again prior to the abrasion experiments. The tray sides were adjusted to the level of the soil to avoid disruption to the near-surface airflow in a non-recirculating suction-type wind tunnel. The wind tunnel was approximately 10 m long, 1.0 m high and 0.5 m wide. The wind profile developed over the first 7.8 m of the tunnel over a fixed roughness. The test section into which the trays were placed occupied the last 2.2 m. The soil trays were mounted in the centre of the wind tunnel. The flow convergence section was 2.5 m long and contained a honeycomb and a fine aluminium insect screen used to strengthen the flow. A fan at the end of the tunnel was powered by an electrical motor to draw air from the work section of the tunnel and generate the air stream. The wind velocity in the tunnel was regulated by controlling the frequency at which the fan rotated. The tunnel was the same as that used in previous agricultural soil experiments (Amante-Orozco and Zobeck, 2002) and is described elsewhere (Amante-Orozco, 2000). An aeolian sediment trap (Big Spring Number Eight; Fryrear, 1986) was located approximately 25 cm downwind of the soil trays and was used to sample the material in transport (abrader material and the eroded soil material). Each tray was initially exposed to a free stream wind velocity of 16 m s⁻¹ (measured at c. 60 cm above the floor of the wind tunnel) for 5 minutes to remove any loose erodible material (LEM). During this time the relative humidity was checked to ensure that it was below 60 per cent to ensure consistency in the relative erodibility of the experiments. The abrader material was then added to the airflow at a rate of 0.28 g cm⁻¹ s⁻¹ and the soil tray was abraded for 1 minute. The soil tray was removed from the tunnel and the on-nadir spectral reflectance was measured as before. It was then returned to the wind tunnel and exposed to an additional 8 minutes of abrasion at the same wind speed and abrasion input rate as before. The soil tray and the wind eroded material were removed from the wind tunnel and measured for on-nadir reflectance for the final time. The on-nadir reflectance of the abrader material was also measured. The experiments were performed in Texas between March and April 2002.

Semi-quantitative analysis of soil spectral reflectance

Most studies that derive soil physical and chemical properties from reflectance are based on empirical relationships between various waveband combinations and the properties of interest. Many authors have shown (e.g. Baumgardner *et al.*, 1985; Ben-Dor *et al.*, 1999; Galvão *et al.*, 2001; Leone and Sommer, 2000) that properties such as organic matter content, moisture content and mineral composition can be determined by examining the spectral response of soils. This can be achieved by examining the intrinsic optical properties of the soil whereby such measurements produce wavelength-specific absorption of electromagnetic radiation, yielding diagnostic reflectance spectra for the properties under investigation.

Some general results from spectroscopy laboratory experiments (Table III) include broad and shallow absorption bands in wavelengths smaller than 1000 nm due to iron-oxide phases (goethite and haematite); narrow and well-defined absorption features at 1400 nm, 1900 nm and 2200 nm related to clay minerals (the presence of moisture reduces the overall soil reflectance but strong absorption features at 1400 nm and 1900 nm remain the same; Obukhov and Orlov, 1964); an increase in organic matter, iron oxides and the clay fraction produces a soil reflectance decrease. Relationships between reflectance and such soil properties have been attempted by Ben-Dor and Banin (1995) and Ben-Dor *et al.* (1997), amongst others.

Heute and Escadafel (1991) identified the five most important soil spectral response functions from a wide genetic range of soil materials. These eigenspectra represented independent sources of spectral variation which in linear combination were able to reconstitute the experimental data. Some of the diagnostic wavebands are also included in

Table III. Nine absorption bands and their main soil components responsible for their position on the reflectance spectra (after Leone and Sommer, 2000)

Absorption bands (nm) (nominal from the literature)	Soil components
488	Goethite
530	Haematite
670	Goethite-haematite
880	Haematite
940	Goethite
1400	Hydroxyl ions and bound water
1900	Hydroxyl ions and bound water
2200	Clay minerals
2300	Calcite

Table III. They identified an eigenspectrum with a slightly sigmoidal curve that represented the mean soil spectral curve and was characterized by brightness. A second eigenspectrum showed absorption at 540 nm and slight (broad) absorption at 820 nm which resembled the spectral behaviour of iron oxides (represented the amount of redness in the soil). Eigenspectrum 3 was concave and resembled the curves of Stoner and Baumgardner (1981) because it was influenced by decomposed organic constituents. The fourth eigenspectrum exhibited characteristics that were similar to the absorption features of goethite, a yellow reduced form of iron oxide around 460 nm and 560 nm. The spectral feature in the 520–600 nm region had the effect of adding or subtracting green to a soil's signature enabling discrimination between the red and yellow forms of free iron oxides in soil. Eigenspectrum 5 identified peaks at 550 nm (minimum at 600 nm) and a broad peak at 770 nm although the authors could not provide an interpretation for this curve.

Canonical ordination (redundancy analysis) of soil spectral reflectance

The canonical form of principal component analysis (PCA) is known as redundancy analysis (RDA) where axes are constrained to linear combinations of external or 'environmental' variables to minimize the sum of squares (ter Braak, 1988). It was used here to establish the relations between reflectance in wavebands (identified in Table III and 460, 560, 770, 820), soil type and soil treatment and is analogous to integrating multiple regression with ordination analysis such as PCA. It is important for the interpretation of the RDA to note that a particular soil type (e.g. FSL) comprised an indicator variable (1 = positive and 0 = negative) of all samples for which seven are positive for that soil type in each soil treatment (Table IV). Similarly, a particular soil treatment (e.g. low rain) comprised an indicator variable for the presence and absence of the treatment for each soil type.

The use of RDA is typically found in ecological analyses and is becoming more common in soil geomorphology (Odeh *et al.*, 1991; Chappell *et al.*, 1996) to extract patterns in the explained variation. To date it has not been applied to remotely sensed data or used to analyse soil reflectance. The program CANOCO (ter Braak, 1988) was used for RDA. The reflectance data were not transformed since they were all in the same units. Samples were standardized and wavebands were centred and standardized. A focus on scaling of inter-sample distances was used to interpret the relationships among reflectance for wavebands from the ordination diagram. The reflectances of each waveband were divided (after extraction of their axes) by their standard deviations so that the ordination diagram displayed standardized reflectance data and correlations instead of covariances. An imaginary vector drawn from the origin of the ordination diagram to each waveband represents the fit (correlation) with the ordination axis. Nominal environmental data are best represented by plotting the centroids of their samples. Similarity between the waveband vectors and those for the centroids of environmental variables quantify the correlation between the two. Imaginary vectors oriented in approximately the same direction indicate strong positive correlation, whilst those oriented in opposite directions imply strong negative correlation; and vectors orthogonal to one another were uncorrelated.

To explain the variation in reflectance for several wavebands and several different soil types of multiple soil treatments, the analysis was performed on all of the soil types and treatments combined and then separately on the soil treatments for each soil type. The most significant predictive variables were selected after the removal of redundant variables with large multicollinearity. A forward selection procedure which used a Monte Carlo permutation test at each selection step was used to test the statistical significance of the variance explained by each variable added to the model (ter Braak, 1988).

Table IV. Indicators of soil types and soil treatments for samples used as 'environmental' variables for redundancy analysis

Sample ID	Soil type			Soil treatment			
	FS	FSL	CL	Low rainfall	High rainfall	Short abrasion	Long abrasion
10	1	0	0	0	0	0	0
11	1	0	0	1	0	0	0
12	1	0	0	1	0	1	0
13	1	0	0	1	0	0	1
14	1	0	0	0	1	1	0
15	1	0	0	0	1	0	0
16	1	0	0	0	1	0	1
20	0	1	0	0	0	0	0
21	0	1	0	1	0	0	0
22	0	1	0	1	0	1	0
23	0	1	0	1	0	0	1
24	0	1	0	0	1	1	0
25	0	1	0	0	1	0	0
26	0	1	0	0	1	0	1
30	0	0	1	0	0	0	0
34	0	0	1	0	1	1	0
35	0	0	1	0	1	0	0
36	0	0	1	0	1	0	1

Linear mixture modelling

Mixture modelling is an established technique that is commonly applied to remotely sensed images to estimate sub-pixel proportions of ground-cover classes (Metternicht and Fermont, 1998). The basic premise is that the pixel composite spectral response is the linear sum of the reflectance measurements of the individual ground components, weighted by their relative proportions. Given that the spectral responses for all specified ground-cover components under conditions of complete coverage of a pixel are known (the so-called end-members) then the linear model can be inverted to estimate the proportions of the ground cover classes within individual pixels.

In this study material trapped in the wind tunnel represented a mixture (M) of two sources (s), the abrader material and the soil surface. If we assume that the spectral reflectance of the mixed material is a linear combination of the sources then their relative proportions (a) can be calculated. Thus, the proportions of the sources were estimated from the mixture using a constrained least-squares solution with equal probability that each source occurred. The basic model is described by:

$$M_n = \sum_s^z (a_{ns}x_s) + e_s \quad (1)$$

where M_n = eroded material reflectance for the n th spectral band; x_s = proportion of the s th source in the eroded material; a_{ns} = end-member of the s th cover type for the n th spectral band; e_n = error term for the n th spectral band; $s = 1, 2, \dots, z$ (number of sources of the eroded material); $n = 1, 2, \dots, z$ (number of spectral bands). The proportion estimates were constrained to be non-negative and to sum to one.

Results

As a reminder, the specific objectives of this paper are to compare the main findings of the soil reflectance literature and the preliminary results of laboratory experiments to (1) examine the composition of three soils using soil reflectance data and (2) characterize soil surface change in composition under controlled rainfall, drying and wind tunnel experiments.

Soil characteristics and visual observations during treatments

The soils used in this investigation were Amarillo fine sand (FS), Amarillo fine sandy loam (FSL), and Randall clay loam (CL). Table I shows the characteristics of the soils. The median particle size represents the particle size distribution

for each soil type. The FS soil is generally coarser, has more sand and lower silt and clay content than the other soil types. The CL soil is generally the finest material, has the least sand and the largest content of silt and clay. The FSL has intermediate amounts of sand and notably similar proportions of clay and silt. The abraded material comprised washed sand and was much coarser than the soils.

The organic carbon content is smallest in soil FS, intermediate in soil FSL and the largest content is found in soil CL. The pH of those soils does not follow the same pattern. That of soil FSL is considerably larger than the other soil types. The pH of soil FS is the next largest, whilst soil CL has the smallest pH. Munsell colour designations are also listed for all soils in Table I. All soils had a brown to strong brown colour with only slight differences in value or chroma. The CL soil had the lowest chroma, with a Munsell colour of 7.5YR 5/2. Soil FS had a slightly stronger brown colour with a higher chroma, 7.5YR 5/6. Soil FSL had the lowest value at 7.5YR 4/4. The abraded material was light grey, with a Munsell colour designation of 10YR 7/2.

The greyscale images taken before the treatments, after rainfall and drying and after abrasion are shown in Figure 1. The untreated soils all appear very similar but there are subtle differences in their brightness. The rainfall treatment seemed to change the brightness of soils, compared to the untreated condition. However, the differences were not great enough to justify changing the Munsell colour designations as listed in Table I. These images (Figure 1) show that the soils are initially similarly unconsolidated and that the surface particles are aggregated in their dry state. Regardless of the rainfall intensity, all soils were crusted, cracked and showed evidence of rainsplash erosion (induced roughness). The CL soil did not exhibit a change in roughness by rainsplash erosion as much as the other soil. After low and high rainfall intensities there appeared to be loose material on the surface of soil FS. After rainfall and drying, soils FS and CL became brighter whilst soil FSL became slightly darker than the original soil surface. The soils exposed to low intensity rainfall appeared to have developed a rougher surface than those exposed to the high intensity rainfall. After abrasion, all soils became slightly darker than those after the previous treatment. The loose erodible material (LEM) on the surface of soil FS was removed. Similar LEM was not present on the surface of the other soils and the surface roughness decreased, presumably as a consequence of the abrasion. The material used as an abradant was deposited on the surface of soil FSL (light grey).

Semi-quantitative analysis of soil on-nadir spectral reflectance

The standard deviation about the mean spectral reflectance for three azimuth angle rotations and three sample replicates for soil type FS is shown in Figure 2. Without exception, the variation in the mean reflectance of soil sample replicates is greater than that of the rotated samples. This is believed to be sufficient evidence for considering only the sample replicate variation in measured soil reflectance. On all subsequent figures this variation was represented by error bars for wavebands selected from the literature (Table III) and additional ones that together were used for the RDA.

The reflectance spectra for the replicate soil samples of each soil type measured before treatment are shown in Figure 3. Also shown is the reflectance spectrum of the material used to abrade the soil surfaces.

The abradant material displays the largest reflectance since the particles appear white. For soil types FS and FSL, there are two spectra which represent the mean reflectance of three replicates that were used in either the high or low rainfall intensity experiment. The error bars located at selected wavebands represent the standard deviation of those replicate reflectances from the mean reflectance. The reflectance spectra of each soil type were significantly different from one another only at wavelengths larger than *c.* 570 nm. This figure provides the baseline for change in the reflectance spectra during the soil treatments. The reflectance spectra from each treatment were subtracted from the reflectance spectrum of the original soil surface. Thus, subsequent spectra indicate difference relative to their original surface and are standardized for all soil types (Figures 4–6).

The reflectance of spectra for all treatments of soil FS relative to the original surface are shown in Figure 4. The spectra of those soil replicates exposed to low rainfall intensity (Figure 4a) show significant differences in reflectance between treatments for wavebands less than *c.* 1000 nm in the visible part of the spectrum (VIS). In this region the low intensity rainfall has produced a bright surface. The abrasion of that surface has reduced the reflectance. As the duration of abrasion increased so the reflectance decreased. Furthermore, the abrasion process has preferentially reduced the reflectance around 690 nm relative to that around 600 nm. In the near-infra-red region (NIR, *c.* 1000–1800 nm) there appears to be no significant difference between the soil reflectance after 8 minutes of abrasion and the original surface. However, the surfaces produced after rainfall and initial (1 minute) abrasion of the surface have much larger reflectance than the original surface. In the shortwave infra-red (SWIR, *c.* 1800–2450 nm) region there is barely any significant difference between the abrasion durations and no significant difference between the low rainfall and the initial abrasion treatments.

The spectra of those soil replicates exposed to high rainfall intensity (Figure 4b) exhibit a very similar pattern of reflectance to those exposed to low rainfall intensity. However, the high rainfall intensity has produced a higher


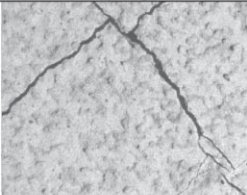
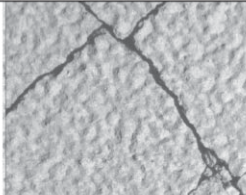

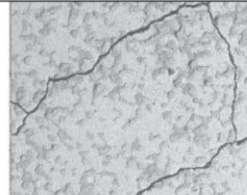
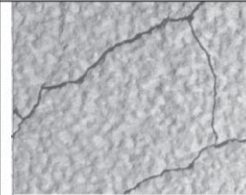

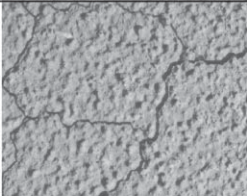


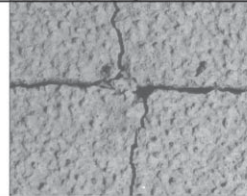
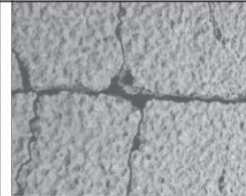





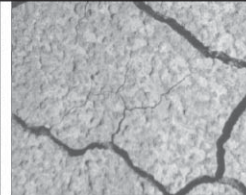
Soil type	Low rainfall intensity			High rainfall intensity		
	Untreated	After rainfall and drying	After 9 minutes aeolian abrasion	Untreated	After rainfall and drying	After 9 minutes aeolian abrasion
FS						
FSL						
CL						

Figure 1. Portions (c. 300 mm × 200 mm) of on-nadir video images taken before treatment, after low and high rainfall intensity and drying treatment and after an accumulated 9 minute aeolian abrasion treatment for each soil type (see text for details).

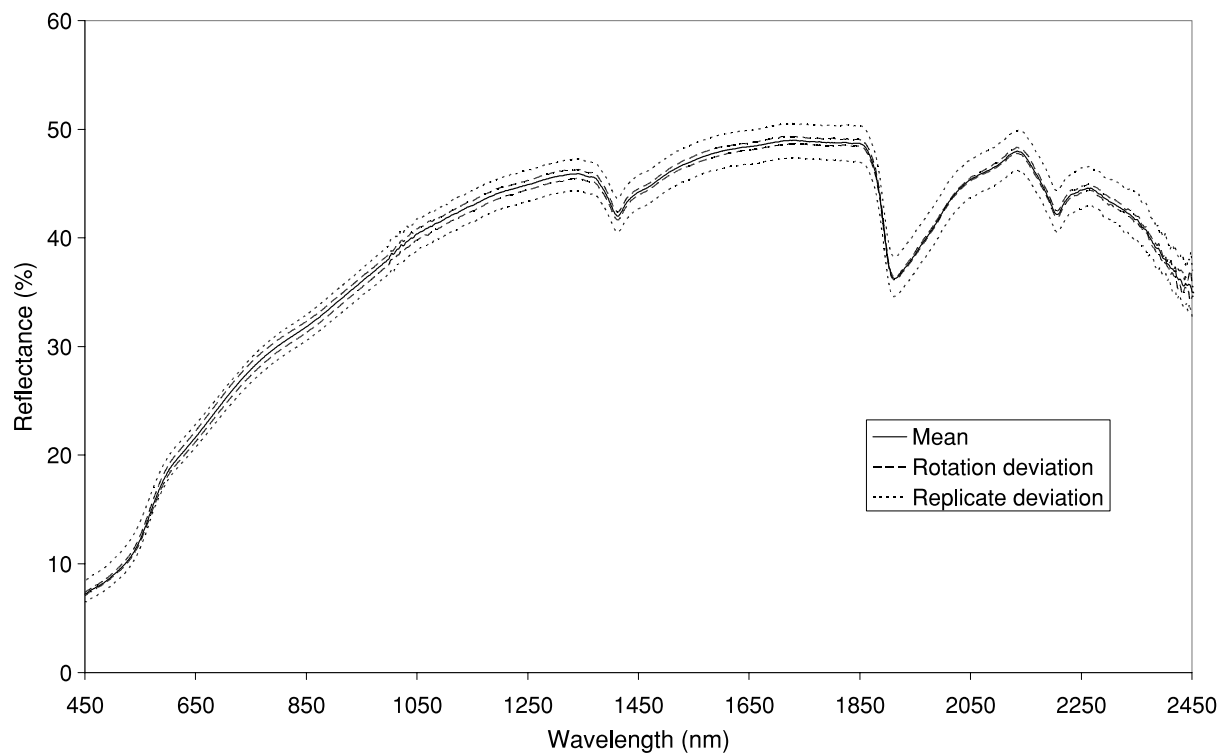


Figure 2. The standard deviation about the mean reflectance measurements for three azimuth angle rotations and three replicate samples of the same soil type.

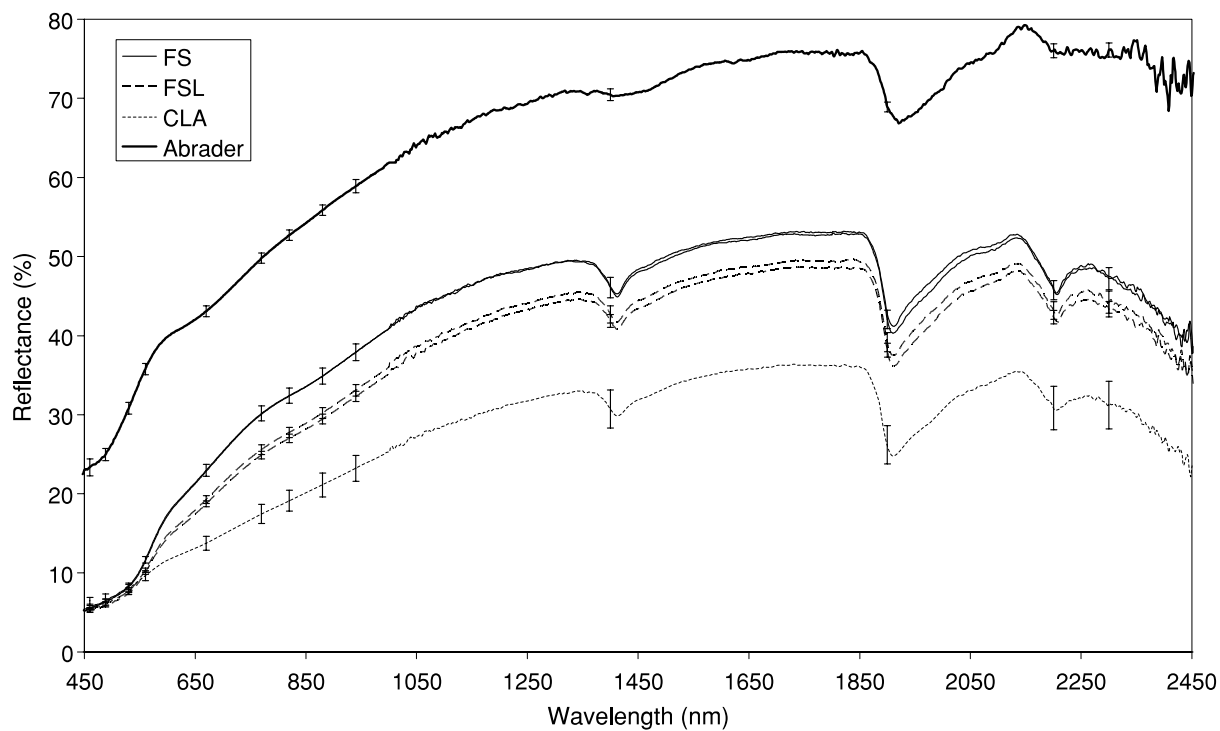


Figure 3. The mean and standard deviation of the spectral reflectance for replicate samples of untreated soils and material used as an abrader.

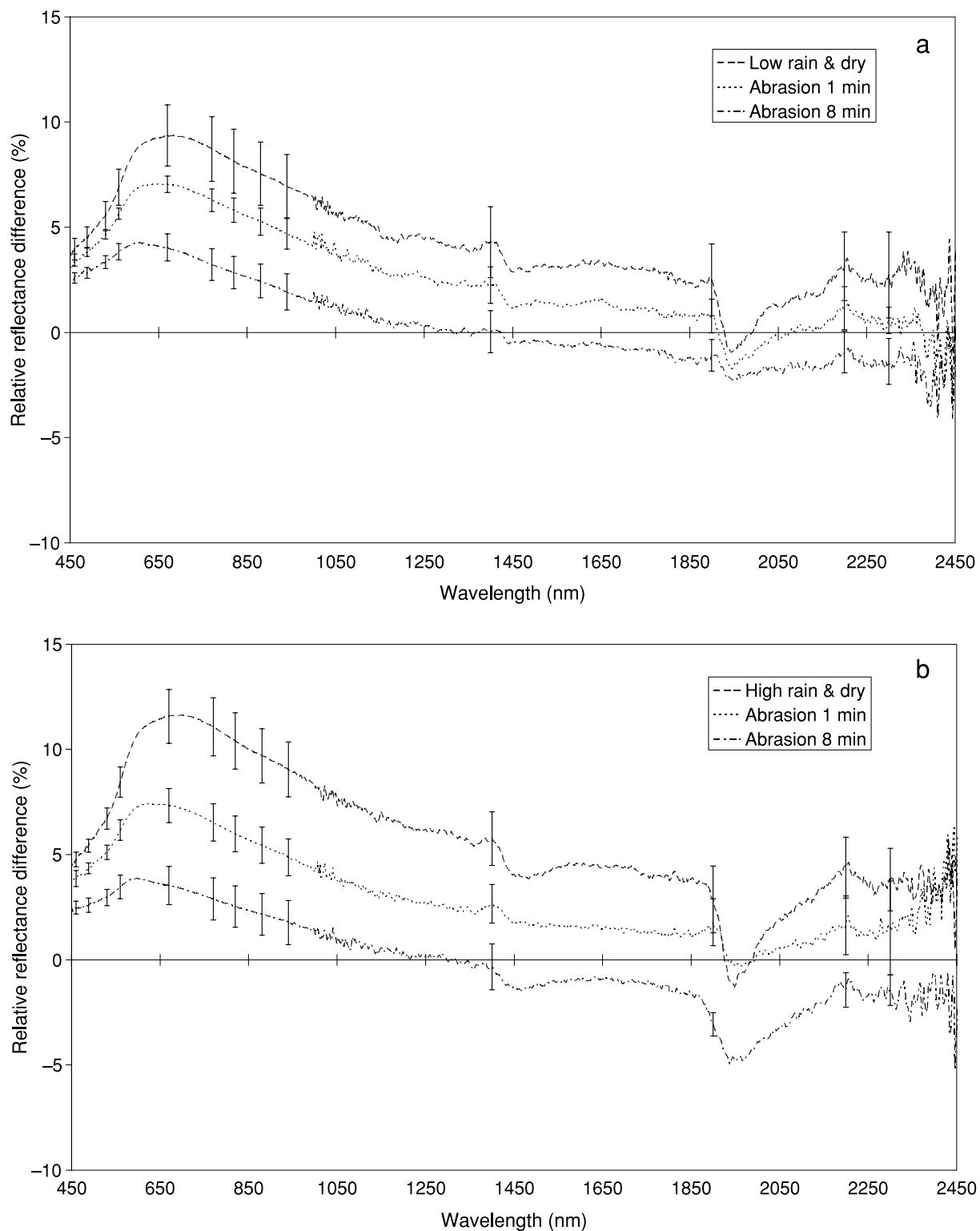


Figure 4. The mean and standard deviation of replicate samples of the spectral reflectance relative to the untreated spectra for soil type FS (see text for details) after low rainfall intensity (a) and high rainfall intensity (b) and aeolian abrasion.

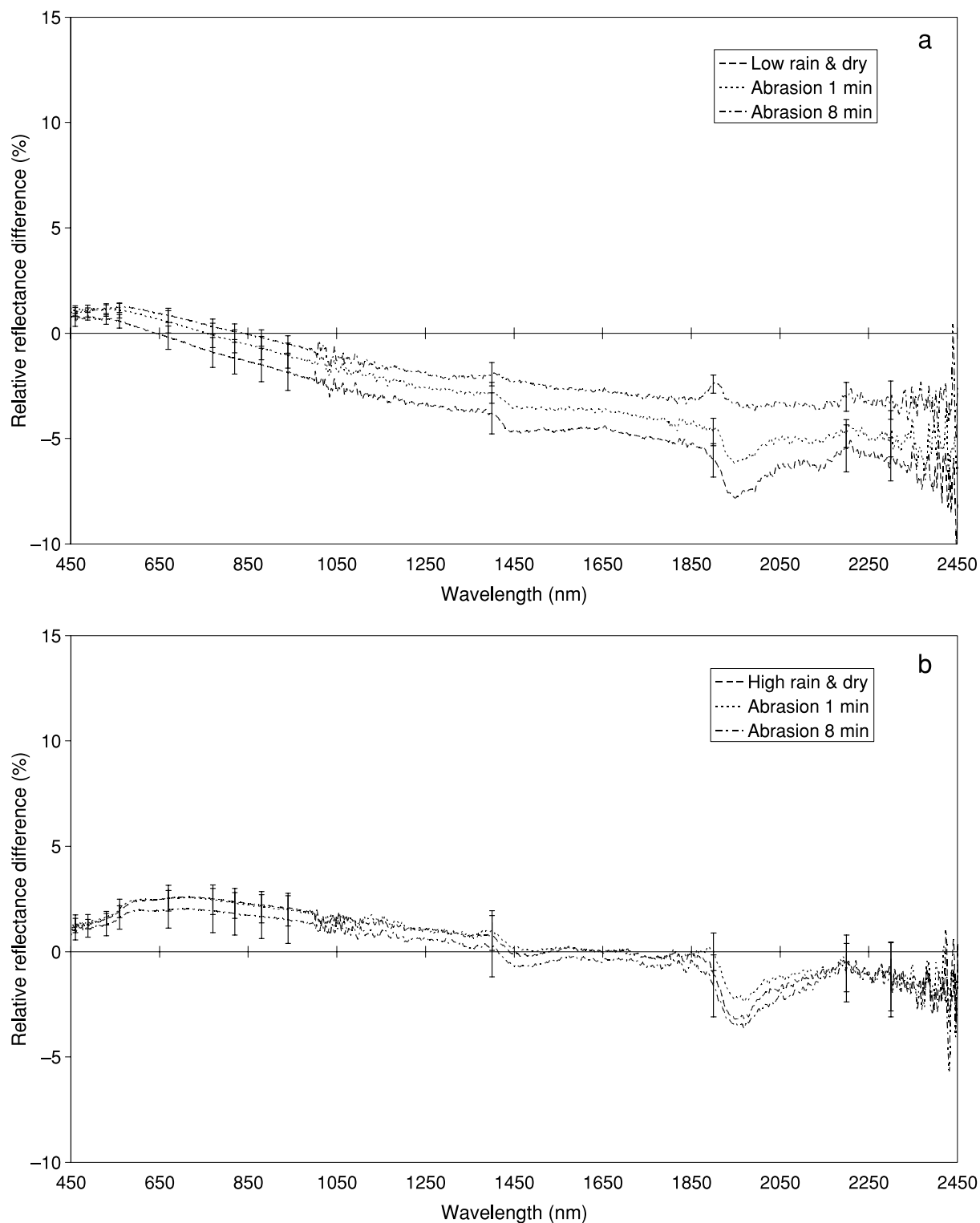


Figure 5. The mean and standard deviation of replicate samples of the spectral reflectance relative to the untreated spectra for soil type FSL (see text for details) after low rainfall intensity (a) and high rainfall intensity (b) and aeolian abrasion.

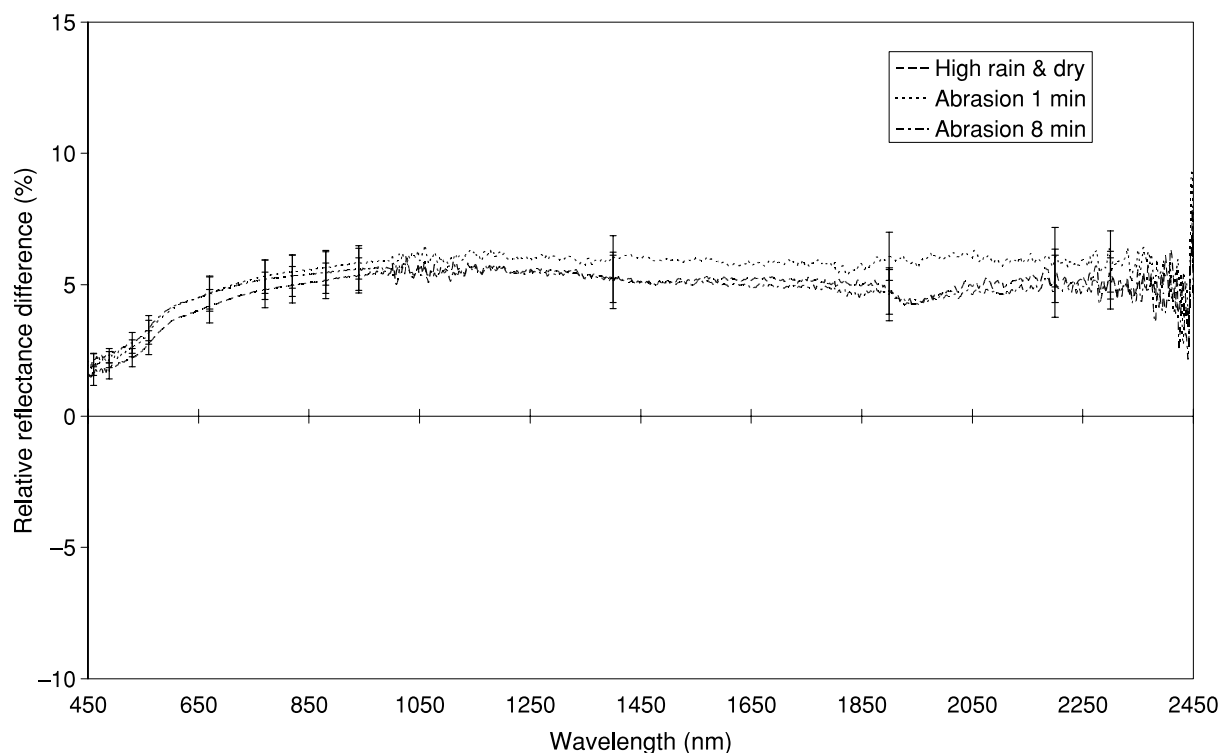


Figure 6. The mean and standard deviation of replicate samples of the spectral reflectance relative to the untreated spectra for soil type CL (see text for details) after high rainfall intensity and aeolian abrasion.

magnitude reflectance in all spectral regions than that of the soil exposed to low rainfall intensity. The spectral features around 1400 nm and 1900 nm for the high rainfall and 8 minute abrasion are much deeper and broader than those of the low rainfall intensity (Figure 4b). The only other significant difference in the spectra between rainfall intensities is that the soil surface treated to high rainfall intensity and subsequently abraded after 8 minutes has a significantly smaller reflectance in the region 1800–2150 nm than the original surface for that rainfall intensity and than the abraded surface for the low rainfall intensity.

In contrast to soil FS, the low intensity rainfall produced a surface for soil FSL (Figure 5a) that was generally darker than the original surface (negative relative differences). The abrasion of that surface increased the reflectance but it remained darker than the original surface. The exception to this generalization is in the VIS region where the reflectance is larger than the original surface. However, many of the wavebands in this region have a magnitude of reflectance that is little different from those of the original surface. There is little separation in the reflectance spectra between treatments. In the NIR region there appears to be a significant difference between spectra for different treatments. In this region it is evident that the rainfall produced the darkest surface and abrasion increased reflectance. This pattern is continued in the SWIR region. However, there are notable features that have arisen during the treatments. The first occurs in this region around 1900 nm in the reflectance spectra for abrasion after 8 minutes. The similarity in relative reflectance between 2030 nm and 2130 nm is due to absorption of reflectance in this region.

The spectra of those FSL soil replicates exposed to high rainfall intensity (Figure 5b) exhibit a pattern of reflectance that is different from those exposed to low rainfall intensity. The treated surfaces are brighter than the original surface throughout the VIS region. Around the start of the NIR region the spectra appear no longer significantly different from the original surface. This is generally the case through the NIR region and into the SWIR region. Without exception there appears to be no significant difference between the reflectance spectra for each treatment. No notable features have arisen in the SWIR region during the treatments.

The high intensity rainfall and abrasion of soil CL (Figure 6) produced a surface that is generally significantly brighter than the original surface throughout the spectra. However, there appears to be no significant difference in the spectral reflectance between treatments. No notable features have arisen in the SWIR region during the treatments.

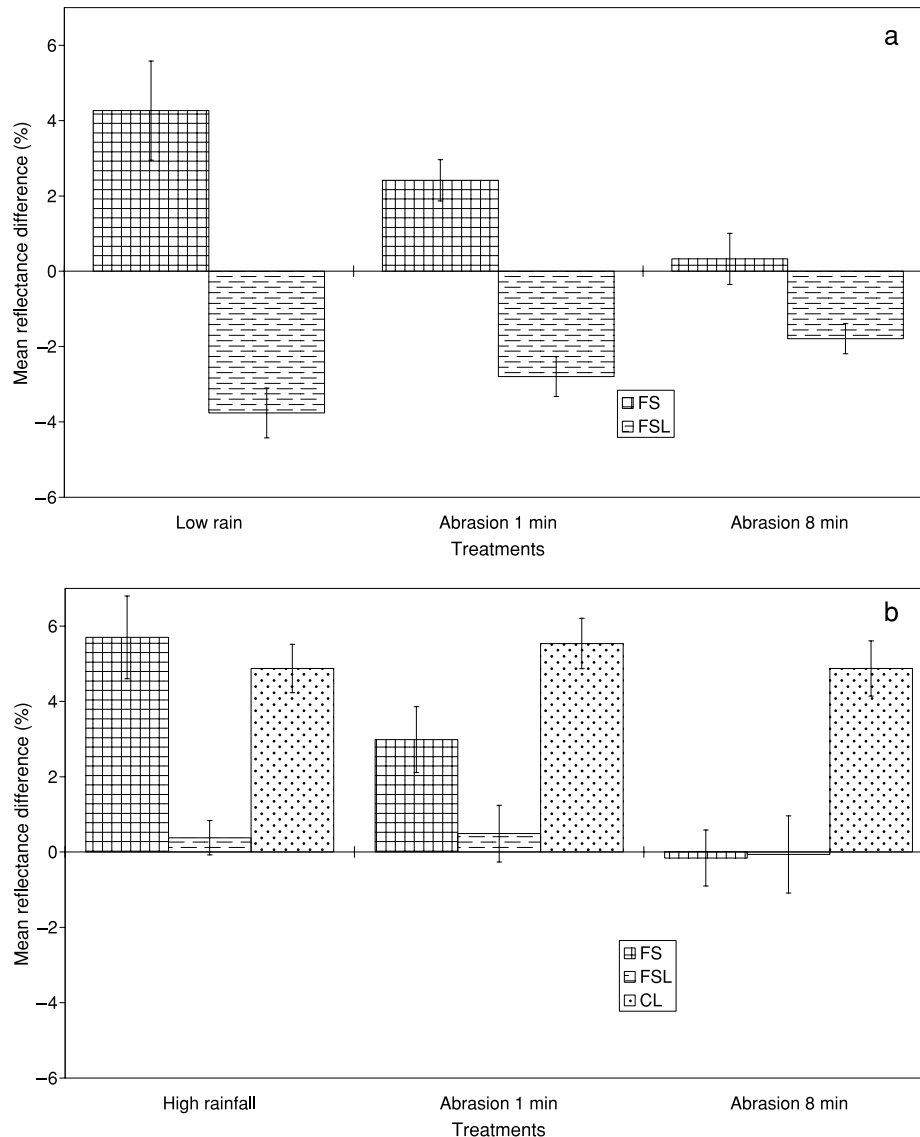


Figure 7. Histograms of the mean difference between the reflectance spectrum for an untreated soil and that after rainfall and abrasion after 1 minute and 8 minutes for each soil type for (a) low intensity rainfall and (b) high intensity rainfall.

A comparison between soils is more complicated and requires some reduction in variation. One way of simplifying the results is to use the mean error or difference between each spectrum and the untreated spectrum. The mean error is sensitive to the bias in the data (either positive or negative) and this indicates the predominant increase or decrease in brightness. The mean error of each soil for each treatment is shown in Figure 7.

Figure 7a shows that soil FS became positively biased after low intensity rainfall indicating an increased brightness that was reduced after abrasion as the reflectance became more similar to that of the untreated soil. The increase in brightness for the same soil after high intensity rainfall (Figure 7b) was larger than that of the soil exposed to low intensity rainfall. Abrasion also reduced the brightness and caused the reflectance of the soil surface to become very similar to that of the untreated soil. Soil FSL decreased in brightness after the low intensity rainfall and following abrasion it increased in brightness and the reflectance tended towards that of the untreated soil. In contrast, the treatments of soil FSL appeared to make little difference between the reflectance of the surface and that of the untreated soil when exposed to high intensity rainfall. Soil CL was only exposed to high intensity rainfall (Figure 7b) and it showed an increased brightness after rainfall but the reflectance remained large after the abrasion treatments.

Canonical ordination (redundancy analysis) of soil spectral reflectance

The results of the redundancy analysis (RDA) are shown in Table V and Figures 8 and 9. The eigenvalues in Table V measure the importance of each of the canonical axes. Table Va provides statistics for the first two canonical axes for analysis of all soil types and treatments and for soils FS and FSL. In the first RDA the first axis explains 63 per cent of the variation whilst the second axis explains 30 per cent. Thus, a considerable amount of the variation in the data is explained by the first two axes. This pattern of explanation is similar to the RDA with soil FS (Table V). The explanation of variance for soil FSL was approximately equivalent in the first two axes. In each of the analyses the relationship between the wavebands and the treatments for each axis is very strong. However, in constrained analysis (such as RDA) a large correlation between these components does not mean that an appreciable amount of the waveband data is explained by the treatment data (ter Braak, 1988). The amount of variation between the wavebands and the treatments is explained by each axis and is given as a cumulative percentage on the bottom line of Table Va. In the case of all soils and treatments 66.2 per cent of the variation is explained by the first axis and the second axis provides only an additional 32.1 per cent. For soil FS more than 90 per cent of the waveband-treatment variance is explained by the first axis leaving only 8 per cent explained by the second axis. This contrasts markedly with soil FSL where the first axis explains approximately 50 per cent and the second axis 40 per cent of the variation.

Figures 8 and 9 provide a visual explanation for these statistics. The wavebands are separated into distinct groups oriented along the axes. In Figure 8, wavebands in the NIR region (in particular 670 nm) are strongly related to the positive direction of axis 1, whilst those of the SWIR region (in particular 2300 nm) are strongly related to the negative direction of the same axis. In contrast, wavebands of the VIS region (in particular 488 nm) are strongly related to the positive direction of the second axis. Thus, two-thirds of the variation in the wavebands may be

Table V. (a) Ordinary RDA with forward selection removal of multicollinear variables to explain the variation in reflectance using soil types and soil treatments. (b) Explained variance, *P*-values and *F* statistics in RDA with forward selection removal of multicollinearity for predicting reflectance (ranked according to the explanation of variance during forward selection)

(a)

	All soils and treatments		Treatments of soil FS		Treatments of soil FSL	
	Axis 1	Axis 2	Axis 1	Axis 2	Axis 1	Axis 2
Eigenvalues	0.63	0.30	0.82	0.07	0.41	0.33
Waveband-treatment correlations	0.97	0.98	0.99	0.69	0.96	0.99
Cumulative percentage variance						
of waveband data	62.50	92.90	82.40	89.60	41.00	73.60
of waveband-treatment relation	66.20	98.30	91.80	99.80	50.40	90.40

(b)

Treatment variables	Explained variance (%)	<i>P</i> -value	<i>F</i> statistic
<i>All soils and treatments</i>			
FS	0.60	0.005	19.78
FSL	0.31	0.005	38.28
Long abrasion	0.01	0.110	2.32
Short abrasion	0.02	0.145	2.18
Low rainfall	0.00	0.620	0.58
High rainfall	0.01	0.435	0.81
<i>Treatments of soil FS</i>			
Long abrasion	0.61	0.045	6.34
Short abrasion	0.24	0.035	4.56
Low rainfall	0.05	0.425	1.01
<i>Treatments of soil FSL</i>			
Long abrasion	0.40	0.045	2.62
Low rainfall	0.31	0.115	3.18
Short abrasion	0.10	0.345	1.14

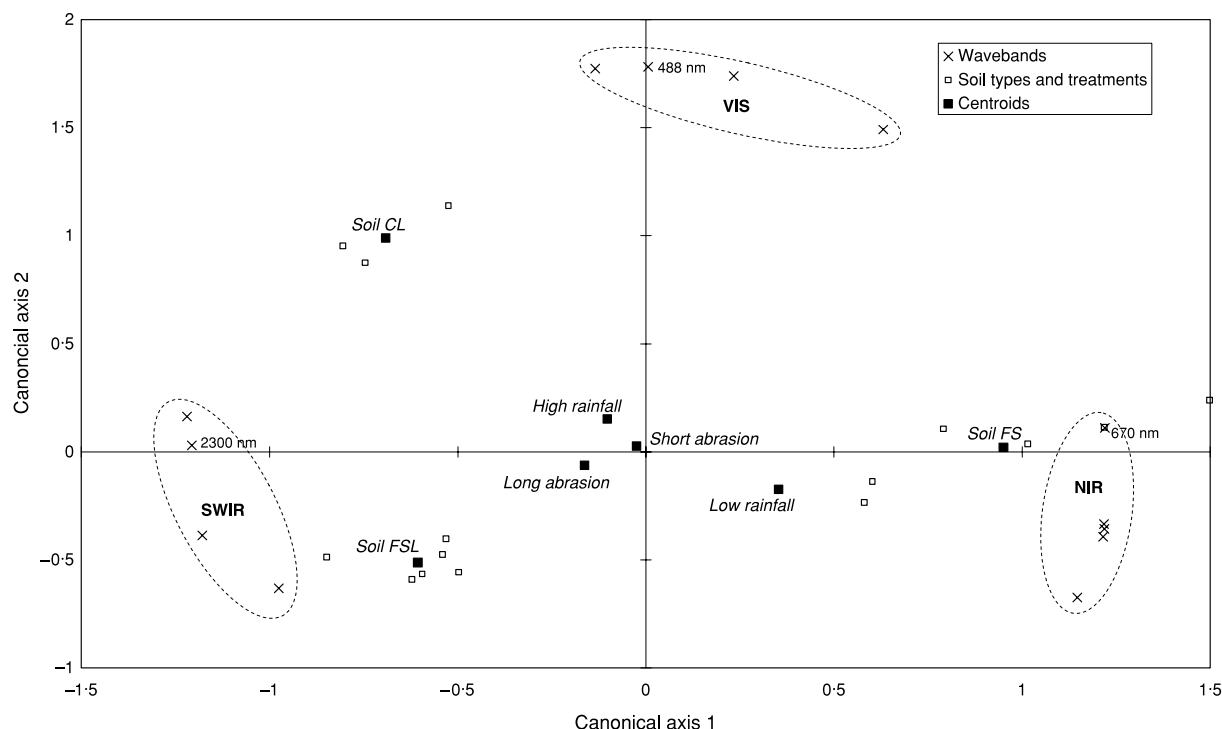


Figure 8. Ordination diagram of redundancy analysis showing the relationships between wavebands in the visible (VIS), near-infrared (NIR) and short-wave infra-red (SWIR) and the ordination axes and the correlations between all soil types and treatments and ordination axes.

explained by canonical axis 1. The soil type centroids are located a greater distance from the origin of the ordination plot than the treatment centroids. Therefore, these centroids explain more of the variation in the axes than do the treatment centroids. Notably, only soil FS is highly correlated with canonical axis 1. Table Vb provides a list of variables and their explanation of variance and significance according to the forward selection process. The uppermost portion of the table provides the results of the treatment and soil types combined. Soil FSL is less well correlated than soil FS but explains a considerable amount of the variation in the axes (Table Vb). Soil CL is located orthogonal to soil FSL and is not strongly related to either axis (Figure 8). This, and its omission from the list of variables that explains variation in the forward selection procedure, suggests that the CL variable is collinear and can be written as a linear combination of the other variables (Table Vb).

The ordination plot of treatments for soil FS (Figure 9a) shows the dominance of canonical axis 1. There exists a strong relationship between wavebands in the VIS and NIR region (in particular 670 nm and 770 nm respectively) and the positive direction of canonical axis 1 coincides with a strong correlation with low intensity rainfall. A strong relationship also exists between wavebands in the SWIR region (in particular 2300 nm) and the negative axis of the same axis, and this coincides with the strong correlation with long duration abrasion. High intensity rainfall treatment is redundant in the explanation of variance for soil type FS and was omitted from Table Vb. The forward selection procedure shows that the duration of abrasion dominates the explanation of variation and that the longest duration of abrasion explains most of the variation (Table Vb).

The ordination plot of treatments for soil FSL (Figure 9b) shows that there is a strong relationship in the positive and negative directions of canonical axis 1 and long duration and short duration abrasion, respectively. The former direction is strongly related to wavebands in the SWIR region (in particular 2200 nm) and the latter direction is related to some wavebands of the NIR region (in particular 940 nm). The positive and negative directions of the second canonical axis are strongly related to the low intensity and high intensity rainfall treatments, respectively. Unfortunately, wavebands of the VIS region and notably the 1400 nm waveband from the SWIR region are not well related to either of the canonical axes. High rainfall intensity treatment was again identified as being redundant in the explanation of variation for soil type FSL and was omitted from the list of variables in the lowest portion of Table Vb. The forward selection procedure shows that the variables of long duration of abrasion and low intensity rainfall together

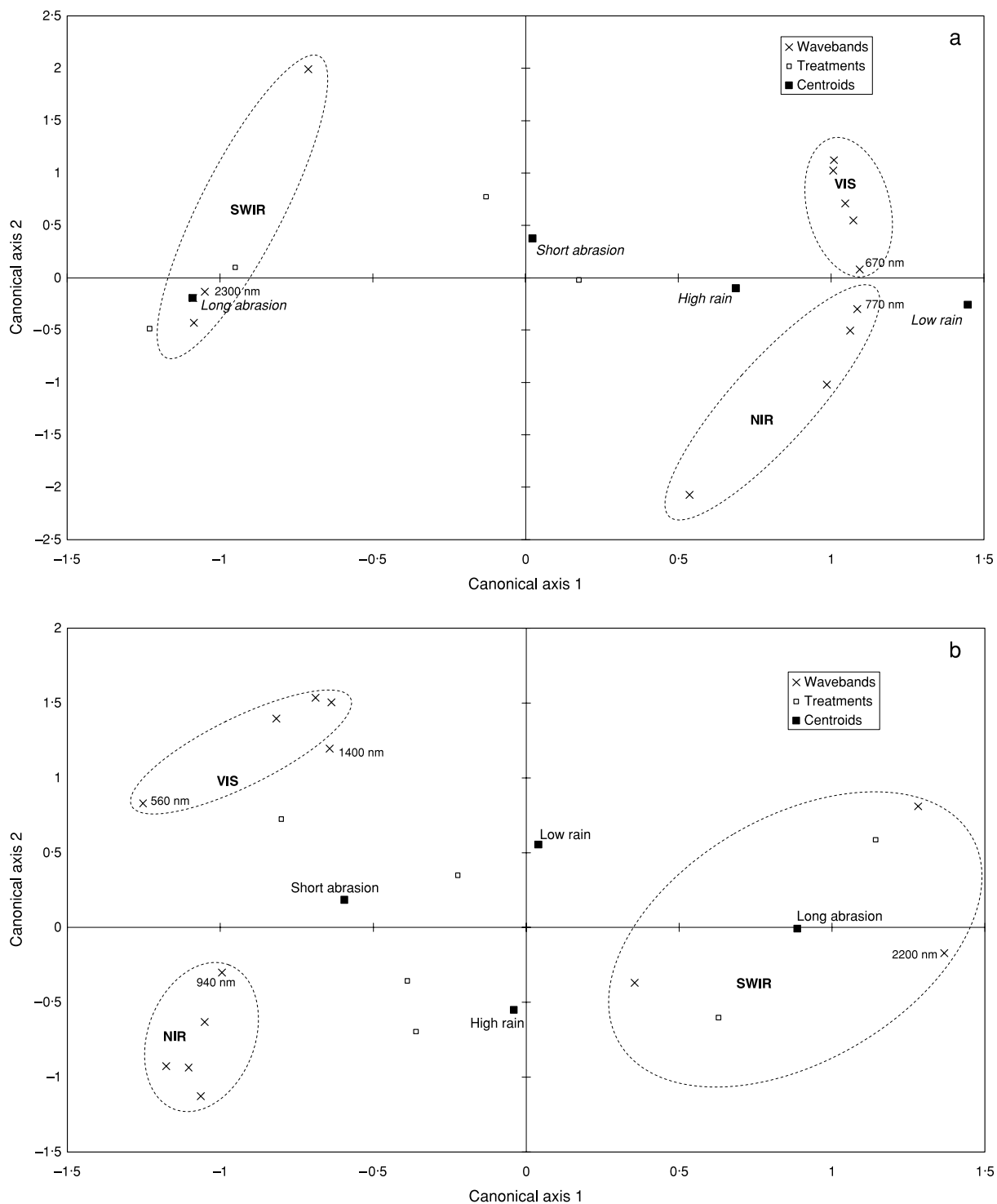


Figure 9. Ordination diagram for redundancy analysis showing the relationships between wavebands in the visible (VIS), near-infra-red (NIR) and short-wave infra-red (SWIR) and the ordination axes and the correlations between treatments and ordination axes within soil types FS (a) and FSL (b).

Table VI. Proportions of the abrader and soil surface (source) material identified from linear mixtures of the eroded material trapped in the wind tunnel

Soil type	Low rainfall		High rainfall		
	FS	FSL	FS	FSL	CL
Abrader	0.32	0.53	0.36	0.72	0.76
Soil	0.68	0.47	0.64	0.28	0.24
Total	1	1	1	1	1

explain more than 70 per cent of the variation. The Monte Carlo tests for significance show that these variables are barely significant at the 5 per cent level (Table Vb).

Unfortunately, there was insufficient data for an ordination analysis of soil CL and treatments.

Linear mixture modelling

Table VI provides a summary of the linear mixture modelling performed on the spectra of eroded material trapped in the wind tunnel, the abrader material and the soil surfaces prior to abrasion. It shows that material eroded from the surface of soil FS contributes most to the trapped material regardless of the intensity of rainfall. In contrast, the high intensity rainfall caused only a small contribution from the surface of soil FSL. The low intensity rainfall produced very similar contributions from the surface of soil FSL and the abrader material. The surface of soil CL contributed very little to the trapped material during abrasion after high intensity rainfall. Notably, this small contribution was similar to that of soil FSL after the same high intensity rainfall treatment.

Discussion

Soil spectral reflectance variation between soil types

The diversity of reflectance among a wide variety of soil samples has been explained by five basic curves: organic-dominated, minimally altered, iron-affected, organic-affected, and iron-dominated (Stoner and Baumgardner, 1981). This approach assumed that each of the observed spectra resulted from one of the five curves using soil properties such as organic matter and iron oxides and that the discriminating factors were slope and presence or absence of absorption bands. The nadir spectral reflectance (Figure 3) and soil properties (Table I) placed the three soils within Stoner and Baumgardner's (1981) minimally altered key curve (Munsell: 10YR 5/3, organic matter 0.59 per cent and iron oxide 0.03 per cent) and that of the iron-affected key curve (Munsell: 7.5YR 5/3, organic matter 1.84 per cent and iron oxide 3.68 per cent). The characteristics of the first key curve was that it had large reflectance, was convex between 500 nm and 1300 nm with strong water features at 1450 nm and 1950 nm and weaker water features at 1200 nm and 1770 nm corresponding to thick water films to fill voids between sand grains. The latter key curve had a slight absorption feature at 700 nm and a stronger feature at 900 nm and a hydroxyl absorption band at 2200 nm. This simple classification suggested that there was little difference in spectral reflectance between the soils as a consequence of their similarity in soil properties (primarily organic matter and iron oxide).

The ordination analyses of all soil types and treatments (Table Va) showed that the majority of the variation in the wavebands was explained by soil types alone. Notably, only soil FS was highly correlated with canonical axis 1 and soil FSL was less well correlated but explained a considerable amount of the variation in the axes (Table Vb). Soil CL was identified as redundant during the forward selection procedure and could be written as a linear combination of the other variables. Variation in soils FS and FSL could be explained by combinations of the NIR (in particular 670 nm) and SWIR wavebands (in particular 2300 nm) and those in the VIS region were orthogonal and unimportant (Figure 8). These results appear to suggest that regardless of the soil surface status a soil may be identified and reconstructed based on key characteristic information. This would be consistent with Stoner and Baumgardner's approach and similar to the results of Price (1990) and more particularly those of Heute and Escadafal (1991). Whilst Stoner and Baumgardner's classification approach may be adapted to yield a more refined result (Kimes *et al.*, 1993) there

remain problems in assigning soils to these classes (Huete and Escadafal, 1991). Ben-Dor *et al.* (1999) illustrated that only subtle differences existed for six soil samples in the SWIR region alone, despite being classified conventionally as distinctly different soil types. They suggested that important information remained hidden in the soil reflectance spectrum. However, we know intuitively that variation of the surface characteristics will cause considerable variation in the spectral reflectance within a soil type. Thus, these results provide a broad explanation of the variation in spectral reflectance that may be explained between soil types. The experiments performed here contained more variation explained by difference in soil type than was explained by soil treatment. This is hardly surprising since the soils were chosen to provide a wide range of responses to a single cycle of treatments (rainfall, drying, abrasion). The broad scale analysis between soil types hides a wealth of information about the soils' responses to treatments.

Erodibility of soil CL

This soil has the lowest erodibility status of all soil types. High intensity rainfall and drying of soil CL increased the brightness of reflectance in all wavebands (Figure 7b). Whilst this response to rainfall was similar to that of soil FS, there were no other similarities between these soils because soil CL showed no significant response to the abrasion treatments. Changes in the brightness of a soil are commonly associated with either differences in moisture status or a change in particle size at the surface (Hunt and Salisbury, 1970; Baumgardner *et al.*, 1985). All soils were dried thoroughly prior to, and between, experiments and therefore we can confidently assign this change in brightness to a difference in particle size at the surface as a consequence of rainsplash. The initial soil surface changed from being unconsolidated to consolidated and sealed. The impact of rainfall at the soil surface caused the preferential movement of particles near the surface of the soil resulting in an upper skin-seal (crust) and deeper wash-in region (McIntyre, 1958). Thus, the orientation of the particles and their distribution on the surface is altered due to rainfall, in this case resulting in an increase in reflectance. Despite the lack of a significant difference in reflectance after abrasion of this soil, the abrasion process removed a little of the material from the soil surface (Table VI). Previous crust studies have shown that abrasion of crusted clay loam soils is usually lower than abrasion of crusted sandier soils (Zobeck, 1991a). Thus, these results indicate that the crust is slightly erodible, but that it is thick and well developed. In other words, the aeolian abrasion, removal of material and consequent surface lowering has not eroded through the surface crust and into the original material.

Erodibility of soil FSL

This soil has an intermediate erodibility status between the other two soils. When exposed to high intensity rainfall and aeolian abrasion this soil was less erodible than when it was exposed to low intensity rainfall and abrasion. High intensity rainfall and drying of soil FSL increased the reflectance only in wavebands of the VIS–NIR region (Figure 7b). In common with the behaviour of soil CL, the increased brightness was ascribed to a change in orientation and distribution of particles at the surface as a consequence of rainsplash. Abrasion of the surface also produced no significant response in the spectra despite material being eroded from the surface (Table VI). Thus, there appears to have been no change in the composition of the soil surface, i.e. there has been no discernible preferential removal, e.g. type or particle size of material. In this case the soil crust was sufficiently well developed that abrasion of its surface made little difference to the surface composition. Although this finding appears to identify the lower limit of surface change detection, before this is positively ascribed it is important to consider changes to the structure of the soil surface (as part of the larger study).

In contrast, after low intensity rainfall soil FSL was observed to become slightly darker (Figure 7a) and this was substantiated by the reflectance spectrum. Notably, the on-nadir image of soil FSL after low intensity rainfall and drying showed more shadow on the surface than on that of the untreated soil and by comparison with the same soil exposed to high intensity rainfall (Figure 7b). The intensity of rainfall appeared to have affected the soil differently. These results are consistent with the findings of Goldshleger *et al.* (2001) and Ben-Dor *et al.* (2003). The less intense rainfall developed erosional features that were emphasized by the illumination and shadow. This demonstrated the importance of roughness on reflectance and its complexity explains the development of models to account for it (Cierniewski, 1987; Jacquemoud *et al.*, 1992; Zobeck *et al.*, 2000; Cierniewski and Karnieli, 2002). The results here indicated that rainfall of high intensity could not sustain the development of similar features in the same soil. Abrasion with two durations of the soil surface produced an increasingly large spectral reflectance indicating an increasingly bright surface (Figure 7a). The digital images showed that the amount of shadow on the soil surfaces decreased due to the abrasion and suggested that the surface roughness also decreased. Thus, the material eroded from the soil comprised the microtopographic highs of the rainsplash-eroded surface. The linear mixture modelling showed that the

eroded material from the crust produced by low intensity rainfall was dominated by material from the soil surface (Table VI). These results are consistent with a previous study which showed that crust abrasion decreased as rainfall intensity increased (Zobeck, 1991a).

Ordination analyses for soil FSL (Table Va) showed that the majority of the variation in the wavebands was explained by two axes and the first axis explained (41 per cent) a similar amount to that of the second axis (33 per cent). The location of the treatment centroids (Figure 9b) shows that the first axis is explained by abrasion and the second axis by rainfall intensity. Furthermore, the longest duration of abrasion is related to variation in the SWIR wavebands (in particular 2200 nm) and to those of the NIR region (in particular 940 nm) and in the VIS region, in decreasing importance. The second axis might reasonably be related to changes in brightness and there are no particular wavebands associated with it (Figure 9b). This interpretation would be consistent with the changes in brightness noted in the reflectance spectra and summarized in the histograms (Figure 7) and the images of the surfaces (Figure 1). Wavebands of the VIS region and notably the 1400 nm waveband from the SWIR region are not well related to either of the canonical axes (Figure 9b). High rainfall intensity treatment is identified as being redundant in the explanation of variation for soil type FSL and was omitted from the analysis (Table Vb). The forward selection procedure shows that the longest durations of abrasion and low intensity rainfall are barely significant and are almost equally important in their explanation of variation during treatment of this soil type (Table Vb).

Erodibility of soil FS

This soil is the most erodible of all soils investigated in this study. When exposed to high intensity rainfall and aeolian abrasion the soil was less erodible than when it was exposed to low intensity rainfall and aeolian abrasion. High intensity rainfall and drying of soil FS increased the reflectance in all but a few wavebands (Figure 7b). In common with the other soils, the change in brightness was ascribed to changes in particle orientation and distribution and, in this case, in the particle size at the surface. The particle size change is the result of the loose erodible material (LEM) that was light in colour, observed on the surface. The LEM was not as evident on the surfaces of the other soils. Initial abrasion of the surface reduced the brightness and this appeared to coincide with the removal of the loose material from the surface (Figure 1). The underlying material appeared smooth and sealed but was evidently more similar in spectral reflectance to the untreated soil than that of the surface after rainfall. However, it is notable that the longest duration of abrasion caused the reflectance in the NIR–SWIR region to decrease below the level of the untreated soil. Based on the visual evidence it is reasonable to assume that the majority of that loose material was eroded. This assumption is validated by the large proportion of eroded material associated with the soil surface reflectance spectrum (Table VI). Removal of the LEM exposed an underlying surface that was different in its reflectance spectrum from that of the untreated soil. This suggests that it had crusted during rainsplash and its reflectance spectrum is similar to that of soil FSL which established a crust. Thus, it appears that the rainsplash surface was created but covered with LEM. This is consistent with the similarity between images for these two soils after abrasion (Figure 1).

The response of soil FS to low intensity rainfall was very similar to that of high intensity rainfall. That response included the presence of LEM at the surface and a similarly patterned surface reminiscent of the rainsplash erosion surface described above. There is an important difference between this soil's response to high and low intensity rainfall. The reflectance spectrum obtained after the longest duration of abrasion was very similar in the NIR–SWIR region to the untreated soil. It showed that the response was not a shift in brightness like the soil's response to abrasion after high intensity rainfall. The results indicate that the large proportion of material eroded from the soil surface (Table VI) was preferentially selected during removal.

Ordination analyses for soil FS (Table Va) showed that the majority of the variation in the wavebands was explained by two axes and the first axis explained (82 per cent) most. The location of the treatment centroids (Figure 9a) shows that the first axis is explained by rainfall in the positive direction and by the longest duration of abrasion in the negative direction. The analysis suggests that the effect of rainfall is removed by the effect of abrasion. This interpretation is consistent with the increased brightness after rainfall regardless of its intensity and the gradual reduction in brightness as a consequence of abrasion (Figure 7). The remaining small amount of variation in the second axis is explained by the shortest duration of abrasion. Furthermore, the longest duration of abrasion is positively correlated with the SWIR wavebands (in particular 2300 nm). The VIS and NIR wavebands (in particular 670 nm and 770 nm respectively) are positively correlated with the rainfall intensity treatments (Figure 9a). High rainfall intensity treatment is identified as being redundant in the explanation of variation for soil type FS and was omitted from Table Vb. The forward selection procedure shows that abrasion dominates the explanation of variance between wavebands and treatment and that the longest duration of abrasion explains most of that variation (Table Vb).

Conclusion

Three soil surfaces were modified using rainfall simulation and wind tunnel abrasion experiments. Observations of those changes were made and recorded using digital images and on-nadir spectral reflectance. The most fundamental finding, important for future work on the erodibility of soil, was the ability to detect the effect of rainfall and abrasion on the surface of a range of soils. The changes detected at the soil surface included the presence of a crust produced by rainsplash, the production of loose erodible material covering a rain crust and the selective erosion of the soil surface. Analysis using on-nadir spectral reflectance allowed the observation of change in the nature of the soil surfaces as inferred using brightness as a consequence of shadowing. Differences in the brightness of the soil surfaces were instrumental in the detection of change. Despite this simplistic data reduction, the results showed clear evidence of the information content in the spectral domain that was otherwise difficult to interpret given the complicated interrelationships between soil composition and structure. Nevertheless, success with this relatively superficial data analysis has important implications for the use of bidirectional spectral reflectance models to quantify the composition and structure of soil surfaces.

From a soil science and geomorphic perspective, the results showed that the effect of rainsplash and aeolian abrasion was different for each soil tested. More specifically, high intensity rainfall produced rain crusts on the soils of clay loam (CL) and fine sandy loam (FSL). Subsequent abrasion of those crusts removed a little of the surfaces and indicated that they were slightly erodible. However, exposure of the FSL soil to low intensity rainfall probably produced a less well compacted rain crust that was abraded at the micro-topographic high elevations and was considerably more erodible than the same soil under high intensity rainfall. The fine sand (FS) soil responded similarly to high and low intensity rainfall. A crust was produced during rainfall but a layer of loose erodible material (LEM) was produced to cover that crust. The LEM was eroded during the abrasion to expose the rain crust. Similar proportions of material were eroded from the soil surface irrespective of rainfall intensity. However, spectral variation in the reflectance of the eroded surfaces suggested that abrasion preferentially removed more material from the FS soil during low intensity rainfall.

Ordination analysis of all soil types and treatments and reflectance data showed that the majority of the variation in the wavebands was explained by soil types alone. The implication is that variation in the spectral reflectance of a soil, irrespective of its soil surface condition, could be explained largely by that of two soil types (FS and FSL). This broad scale of explanation appeared to require reflectance from combinations of the NIR (in particular 670 nm) and SWIR wavebands (in particular 2300 nm) and that those in the VIS region were unimportant. Ordination analyses within each of those two important soil types explained significant amounts of the variation in the reflectance of all waveband regions by treatments of the soil and hence changes in the soil surface. Amongst other things, these analyses suggest a source of considerable variation in spectral reflectance that has hitherto been largely ignored. Laboratory soil experiments designed to develop models for natural environment predictions are likely to be biased by their exclusion of surface conditions for each soil type. It is unreasonable to assume that variation of the surface characteristics will not cause considerable variation in the spectral reflectance within a soil type. Thus, it is likely that the variation in environmental treatments within a soil type is a simple and underestimated source of variation in the characterization of soil surface erodibility and in the remote sensing of soil.

Acknowledgements

This work was funded by an award to A.C. from the UK Natural Environmental Research Council (NER/M/S/2001/00124). The authors are grateful to the United States Department of Agriculture, Agricultural Research Service, for making available the spectroradiometer and the rainfall simulator used in these experiments and to Texas Tech University for generously providing access to the wind tunnel. We are grateful to Dean Holder for constructing the goniometer and for technical assistance with the operation of the wind tunnel and to the two anonymous referees for their comments on the manuscript.

References

- Amante-Orozco A. 2000. *Fine particulate matter generation under controlled laboratory and wind tunnel conditions*. PhD dissertation, Texas Tech University, Lubbock.
- Amante-Orozco A, Zobeck TM. 2002. Clay and Carbonate Effect on Fine Dust Emissions as Generated in a Wind Tunnel. In *Proceeding of the ICAR5/GCTE-SEN Joint Meeting*, Lee JA, Zobeck TM (eds). 22–25 July 2002, Lubbock, Texas; 83–86.
- Baumgardner MF, Silva LF, Biehl LL, Stoner ER. 1985. Reflectance properties of soils. *Advances in Agronomy* **38**: 1–44.
- Baumhardt RL, Romkens MJM, Whisler FD, Parlange JY. 1990. Modeling infiltration into a sealing soil. *Water Resources Research* **26**: 2497–2505.

- Ben-Dor E, Banin A. 1995. Near infra-red analysis (NIRA) as a rapid method to simultaneously evaluate several soil properties. *Soil Science Society of America Proceedings* **59**: 364–372.
- Ben-Dor E, Inbar Y, Chen Y. 1997. The reflectance spectra of organic matter in the visible near infrared and short wave region (400–2500 nm) during a controlled decomposition process. *Remote Sensing of Environment* **61**: 1–15.
- Ben-Dor E, Irons JR, Epema, G. 1999. Soil reflectance. In *Remote Sensing for the Earth Sciences*, Vol. 3. Renz AN (ed.). Wiley: New York; 111–188.
- Ben-Dor E, Goldshleger N, Benyamini Y, Agassi M, Blumberg DG. 2003. The spectral reflectance properties of soil structural crusts in the 1.2 to 2.5 μm spectral region. *Soil Science Society of America Proceedings* **67**: 289–299.
- Böhner J, Schäfer W, Conrad O, Gross J, Ringeler A. 2003. The WEELS model: methods, results and limitations. *Catena* **52**(4): 289–308.
- Burgess RC, McTainsh GH, Pitblado JR. 1989. An index of wind erosion in Australia. *Australian Geographical Studies* **27**: 98–110.
- Chappell A, Oliver MA, Warren A, Agnew CT, Charlton M. 1996. Examining the factors controlling the spatial scale of variation in soil redistribution processes from south-west Niger. In *Advances in Hillslope Processes*, Anderson MG, Brooks SM (eds). J. Wiley & Sons: Chichester; 429–449.
- Chappell A, McTainsh G, Leys J, Strong C. 2003. Using geostatistics to elucidate temporal change in the spatial variation of aeolian sediment transport. *Earth Surface Processes and Landforms* **28**: 567–585.
- Cierniewski J. 1987. A model for soil surface roughness influence on the spectral response of bare soils in the visible and near-infrared range. *Remote Sensing of Environment* **23**: 97–115.
- Cierniewski J, Karnieli A. 2002. Virtual surfaces simulating the bidirectional reflectance of semiarid soils. *International Journal of Remote Sensing* **23**(19): 4019–4037.
- Fryrear DW. 1986. A field dust sampler. *Journal of Soil and Water Conservation* **41**(2): 117–120.
- Fryrear DW, Saleh A, Bilbro JD, Schomberg HM, Stout JE, Zobeck TM. 1998. Revised Wind Erosion Equation (RWEQ). Wind Erosion and Water Conservation Research Unit, USDA-ARS, Southern Plains Area Cropping Systems Research Laboratory. Technical Bulletin No. 1. <http://www.csrl.ars.usda.gov/wewc/rweq.htm>.
- Galvão LS, Pizarro MA, Epiphany JCN. 2001. Variations in reflectance of tropical soils: Spectral-chemical composition relationships from AVIRIS data. *Remote Sensing of Environment* **75**: 245–255.
- Geeves GW, Leys JF, McTainsh GH. 2000. Soil erodibility. In *Soils, Their Properties and Management*, Charman PE, Murphy B (eds). Oxford University Press: New York; 205–220.
- Gillette DA, Hanson KJ. 1989. Spatial and temporal variability of dust production caused by wind erosion in the United States. *Journal of Geophysics Research* **94D**: 2197–2206.
- Goldshleger N, Ben-Dor E, Benyamini Y, Agassi M, Blumberg DG. 2001. Characterization of soil's structural crust by spectral reflectance in the SWIR region (1.2–2.5 μm). *Terra Nova* **13**: 12–17.
- Hagen LJ, Zobeck TM, Skidmore EL, Elminyaw I. 1995. *WEPS technical documentation: soil submodel*. SWCS WEPP/WEPS Symposium. Ankeny, IA.
- Huete AR, Escadafal R. 1991. Assessment of biophysical soil properties through spectral decomposition techniques. *Remote Sensing of Environment* **35**: 149–159.
- Hunt GR, Salisbury JW. 1970. Visible and near infrared spectra of minerals and rocks: I. Silicate minerals. *Modern Geology* **1**: 283–300.
- Irons JR, Weismiller RA, Petersen GW. 1989. Soil reflectance. In *Theory and Applications of Optical Remote Sensing*, Asrar G. (ed.). Wiley: New York; 66–106.
- Jacquemoud S, Bater F, Hanocq JF. 1992. Modeling spectral and bidirectional soil reflectance. *Remote Sensing of Environment* **41**: 123–132.
- Kalma JD, Speight JG, Wasson RJ. 1988. Potential wind erosion in Australia: A continental perspective. *Journal of Climatology* **8**: 411–428.
- Karnieli A, Kidron GJ, Glaesser C, Ben-Dor E. 1999. Spectral characteristics of cyanobacteria soil crust in semi-arid environments. *Remote Sensing of Environment* **69**: 67–75.
- Kimes DS, Irons JR, Levine ER, Horning NA. 1993. Learning class discriminations from a database of spectral reflectance of soil samples. *Remote Sensing of Environment* **43**: 161–169.
- Latz KRA, Weismiller GE, Van Scoyoc GE, Baumgardner MF. 1984. Characteristic variations in spectral reflectance of selected eroded Alfisols. *Soil Science Society of America Journal* **48**: 1130–1134.
- Leone AP, Sommer S. 2000. Multivariate analysis of laboratory spectra for the assessment of soil development and soil degradation in the southern Apennines (Italy). *Remote Sensing of Environment* **72**: 346–359.
- Martcorena B, Bergametti G. 1995. Modeling the atmospheric dust cycle: 1. Design of a soil-derived dust emission scheme. *Journal of Geophysical Research* **100**(D8): 16415–16430.
- McIntyre DS. 1958. Soil splash and the formation of surface crusts by raindrop impact. *Soil Science* **85**: 261–266.
- McTainsh GH, Lynch AW, Burgess RC. 1990. Wind erosion in Australia. *Australian Journal of Soil Research* **28**: 323–339.
- McTainsh GH, Lynch AW, Tews K. 1998. Climatic controls upon dust storm occurrence in eastern Australia. *Journal of Arid Environments* **39**: 457–466.
- Metternicht GI, Fermont A. 1998. Estimating erosion surface features by linear mixture modelling. *Remote Sensing Environment* **12**: 1887–1903.
- Milton EJ, Rollin EM, Emry DR. 1995. Advances in field spectroscopy. In *Advances in Environmental Remote Sensing*, Danson FM, Plummer SE (eds). Wiley: Chichester; 9–32.
- Nickling WG, Gillies JA. 1993. Dust emission and transport rates, Mali, west Africa. *Sedimentology* **40**: 859–868.
- Nickling WG, McTainsh GH, Leys JF. 1999. Dust emissions from the Channel Country of western Queensland, Australia. *Zeitschrift für Geomorphologie* **116**: 1–17.

- Nicodemus FE, Richmond JC, Hsia JJ, Ginsberg IW, Limperis T. 1977. *Geometrical considerations and nomenclature for reflectance*. National Bureau of Standards Monograph No. 160. US Government Printing Office: Washington, D.C.
- Norton LD, Brown LC. 1992. Time-effect on water erosion for ridge tillage. *Transactions of the American Society of Agricultural Engineers* **35**: 473–478.
- Obukhov AI, Orlov DC. 1964. Spectral reflectance of the major soil groups and the possibility of using diffuse reflectance in soil investigations. *Soviet Soil Science* **2**: 174–184.
- Odeh IOA, Chittleborough DJ, McBratney AB. 1991. Elucidation of soil-landform inter-relationships by canonical ordination analysis. *Geoderma* **49**: 1–32.
- Potter KN, Zobeck TM, Hagen LJ. 1990. A micro-relief index to estimate soil erodibility by wind. *Transactions of the American Society of Agricultural Engineers* **33**(1): 151–155.
- Price J. 1990. On the information content of soil reflectance spectra. *Remote Sensing of Environment* **33**: 113–121.
- Shao Y, Leslie LM. 1997. Wind erosion prediction over the Australian continent. *Journal of Geophysical Research* **102**(D25): 30091–30105.
- Shao Y, Raupach MR, Leys JF. 1996. A model for prediction aeolian sand drift and dust entrainment on scales from paddock to region. *Australian Journal of Soil Research* **34**: 309–342.
- Sokolik IN, Toon OB. 1996. Direct radiative forcing by anthropogenic airborne mineral aerosols. *Nature* **381**: 681–683.
- Stoner ER, Baumgardner MF. 1981. Characteristic variations in reflectance of surface soils. *Soil Science Society of America Journal* **45**: 1161–1165.
- ter Braak CJF. 1988. *CANOCO: A FORTRAN Program for Canonical Community Ordination by [partial] [detrended] [canonical] Correspondence Analysis and Redundancy Analysis (version 2.1)*. Agricultural Mathematics Group: Wageningen, The Netherlands.
- Woodruff NP, Siddoway FH. 1965. A wind erosion equation. *Soil Science Society of America Proceedings* **29**(5): 602–608.
- Zobeck TM. 1991a. Abrasion of crusted soils: Influence of abrader flux and soil properties. *Soil Science Society of America Proceedings* **55**: 1091–1097.
- Zobeck TM. 1991b. Soil properties affecting wind erosion. *Journal of Soil and Water Conservation* **46**(2): 112–118.
- Zobeck TM. 2003. Rapid particle size analyses using laser diffraction. American Society of Agricultural Engineering paper no. 032207. Proceedings of the Annual International Meeting of ASAE: Las Vegas, NV.
- Zobeck TM, Popham TW, Mauget SA, Wanjura DF, Upchurch DR. 2000. Using soil surface reflectance to estimate roughness parameters. *Proceedings of the International Soil Tillage Research Organisation* (published on CD).